

Graviton production in anti-de Sitter braneworld cosmology: A fully consistent treatment of the boundary condition

Marcus Ruser, Ruth Durrer, Marc Vonlanthen and Peter Wittwer
*Université de Genève, Département de Physique Théorique,
24 quai Ernest Ansermet, CH-1211 Genève 4, Switzerland*

(Dated: April 14, 2009)

In recent work by two of us, [Durrer & Ruser, PRL **99**, 071601 (2007); Ruser & Durrer PRD **76**, 104014 (2007)], graviton production due to a moving spacetime boundary (braneworld) in a five dimensional bulk has been considered. In the same way as the presence of a conducting plate modifies the electromagnetic vacuum, the presence of a brane modifies the graviton vacuum. As the brane moves, the time dependence of the resulting boundary condition leads to particle creation via the so called 'dynamical Casimir effect'. In our previous work a term in the boundary condition which is linear in the brane velocity has been neglected. In this work we develop a new approach which overcomes this approximation. We show that the previous results are not modified if the brane velocity is low.

PACS numbers: 98.80Cq, 04.50+h

Keywords: Braneworlds, dynamical Casimir effect, graviton production

I. INTRODUCTION

The idea that our Universe is a $3 + 1$ dimensional membrane in a higher dimensional 'bulk' spacetime has opened new exciting prospects for cosmology, for reviews see [1, 2]. In the simplest braneworlds motivated by string theory, the standard model particles are confined to the brane and only the graviton can propagate in the bulk. Of particular interest is the Randall-Sundrum (RS) model [3, 4], where the bulk is 5-dimensional anti-de Sitter space. If the so called RS fine tuning condition is satisfied, it can be shown that gravity on the brane 'looks 4-dimensional' at low energies.

Within this model, cosmological evolution can be interpreted as the motion of the physical brane, i.e. our Universe, through the 5d bulk, acting as a moving boundary for bulk fields, in particular for 5d gravitational perturbations. Such a time-dependent boundary does in general lead to particle production via the dynamical Casimir effect [5, 6].

Of course one can always choose coordinates with respect to which the brane is at rest, e.g. Gaussian normal coordinates. This leads to a time dependent bulk resulting in the same effect, particle production from vacuum due to a time varying background metric. But then, usually (except in the case of de Sitter expansion on the brane [7]), the perturbation equation describing the evolution of gravitons is not separable and can only be treated with numerical simulations [8, 9, 10]. Furthermore, in a time dependent bulk, a mode decomposition is in general ambiguous and one cannot split the field in a zero mode and Kaluza-Klein (KK) modes in a unique way. One of the advantages of the dynamical Casimir effect approach presented in [11, 12] is that it allows for a clear physical interpretation and in addition exhibits an analogy with quantum electrodynamics.

Based on the picture of a moving brane in AdS₅, we have studied graviton production in an ekpyrotic type

scenario [13] where our Universe first approaches a second static brane. After a 'collision' the physical brane reverses direction and moves away from the static brane, see Fig. 1. For an observer on the brane, the first phase corresponds to a contracting Universe, the collision represents the 'Big Bang' after which the Universe starts expanding (see Fig. 1). We do not model the details of this collision, but assume that the brane distance is still finite at the collision. This corresponds to a cutoff of all the physics which happens at scales smaller than the minimal brane distance when contraction reverses into expansion. In our results we assume this to be of the order of the string scale. We cut off the spectra at the string scale. This is a conservative assumption which signifies that we neglect all the particle creation at energies higher than this scale.

We have obtained the following important results in our previous papers [11, 12]: first of all, the energy density of KK gravitons in AdS₅ scales like stiff matter, $\propto a^{-6}$, where a denotes the scale factor introduced in Eq. (2). Therefore, KK gravitons in AdS₅ cannot represent the dark matter in the Universe¹. We have also seen that in the early Universe the back reaction from KK gravitons on the bulk geometry is likely to be important. Finally, we have derived a limit for the maximal brane velocity, the bounce velocity, $v_b \lesssim 0.2$ in order not to over-produce zero-mode (i.e. 4d) gravitons, the energy density of which is constrained by the nucleosynthesis bound. We have also calculated the spectra of both, the zero-mode and the KK gravitons.

In this previous work we have, however, neglected a term linear in the brane velocity v in the boundary conditions (junction conditions) for the tensor perturbations. Here we derive a method which includes this

¹ See [14] for a discussion on a contradicting result in the literature.

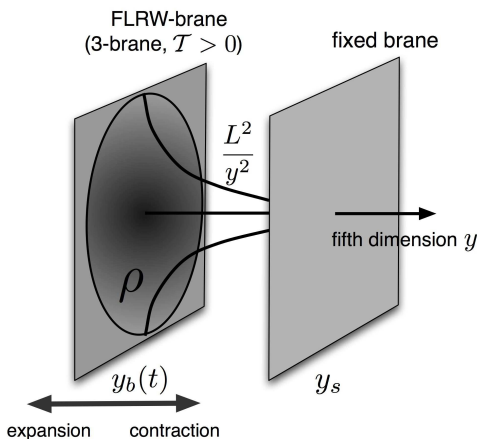


FIG. 1: Two branes in an AdS₅ spacetime. The physical brane, a Friedmann universe with energy density ρ is on the left. While it is approaching the static brane its scale factor is decreasing, the Universe is contracting, and when it moves away from the static brane the Universe is expanding. L is the AdS curvature radius which is related to the brane tension \mathcal{T} via Eq. (8). The value of the scale factor of the brane metric as a function of the extra dimension y is also indicated.

term and allows to treat the problem without any low velocity approximation. We show that the low velocity results previously obtained are not modified. Especially, the nucleosynthesis bound on the maximal brane velocity, $v_b < 0.2$, remains valid. In a subsequent study we shall investigate graviton production from branes which achieve high velocities in detail [15].

The paper is organized as follows. In the next section we repeat the basic equations for the evolution of tensor perturbations (gravitons) and we explain why it is not straight forward to include the velocity term of the boundary condition. In Section III we present the new approach and obtain the modified perturbation equations via a coordinate transformation which is such that the velocity term in the boundary condition disappears. We then quantize the system in the new coordinates. In Section IV we show numerical results for graviton production at relatively low velocities. In Section V we conclude. Technical details are deferred to appendices.

II. A MOVING BRANE IN AdS₅

A. The background

In Poincaré coordinates $(x^A) = (t, \mathbf{x}, y)$ with $\mathbf{x} = (x^1, x^2, x^3)$ and $A = 0, \dots, 4$, the AdS₅ (bulk) metric is given by

$$ds^2 = g_{AB} dx^A dx^B = \frac{L^2}{y^2} [-dt^2 + \delta_{ij} dx^i dx^j + dy^2] , \quad (1)$$

where $i, j = 1, 2, 3$ and L is the AdS₅ curvature radius which is related to the bulk cosmological constant by the 5d Einstein equation, $-\Lambda = 6/L^2$. The physical brane representing our (spatially flat) Universe is located at some time dependent position $y = y_b(t)$ in the bulk, and the metric induced on the brane is the Friedman-Robertson-Walker metric

$$ds^2 = a^2(\eta) [-d\eta^2 + \delta_{ij} dx^i dx^j] , \quad (2)$$

with scale factor $a(\eta)$ which is given by the brane position,

$$a(\eta) = \frac{L}{y_b(t)} . \quad (3)$$

The conformal time η of an observer on the brane, is related to the bulk time t via

$$d\eta = \sqrt{1 - v^2} dt \equiv \gamma^{-1} dt . \quad (4)$$

Here we have introduced the brane velocity

$$v \equiv \frac{dy_b}{dt} = -\frac{LH}{\sqrt{1 + L^2 H^2}} \quad \text{and} \quad \gamma = \frac{1}{\sqrt{1 - v^2}} . \quad (5)$$

H is the usual Hubble parameter,

$$H \equiv \frac{1}{a^2} \frac{\partial a}{\partial \eta} \equiv a^{-1} \mathcal{H} = -L^{-1} \gamma v . \quad (6)$$

Its dynamics, as a result of the second junction condition, is determined by the modified Friedmann equation [1]

$$H^2 = \frac{\kappa_4 \rho}{3} \left(1 + \frac{\rho}{2\mathcal{T}} \right) , \quad (7)$$

where \mathcal{T} is the brane tension, ρ the energy density on the brane, and we assume the RS fine tuning condition [3]

$$\frac{\kappa_5^2 \mathcal{T}^2}{12} = \frac{3}{L^2} . \quad (8)$$

Furthermore (see [3]),

$$\kappa_4 = 8\pi G_4 = \frac{\kappa_5^2 \mathcal{T}}{6} . \quad (9)$$

We define the string and Planck scales by

$$\kappa_5 = \frac{1}{M_5^3} = L_s^3 , \quad \kappa_4 = \frac{1}{M_{\text{Pl}}^2} = L_{\text{Pl}}^2 . \quad (10)$$

Note that the RS fine-tuning condition is equivalent to

$$\kappa_5 = \kappa_4 L \quad \text{or} \quad \frac{L_s}{L} = \frac{L_{\text{Pl}}^2}{L_s^2} . \quad (11)$$

Identifying κ_5 with the string scale is based on the assumption that this phenomenological model comes from string theory with one large extra-dimension L , the y direction, while all the other extra-dimensions remain of the order of the string scale, L_s . In this case the 4d observed Planck scale is related to the string scale by Eq. (11).

B. Tensor perturbations

Allowing for tensor perturbations $h_{ij}(t, \mathbf{x}, y)$ of the spatial three-dimensional geometry at fixed y , the perturbed bulk metric reads

$$ds^2 = \frac{L^2}{y^2} [-dt^2 + (\delta_{ij} + 2h_{ij})dx^i dx^j + dy^2] . \quad (12)$$

Tensor modes satisfy the traceless and transverse conditions, $h_i^i = \partial_i h_j^j = 0$. These conditions imply that h_{ij} has only two independent degrees of freedom, the two polarization states $\bullet = \times, +$. We decompose h_{ij} into spatial Fourier modes,

$$h_{ij}(t, \mathbf{x}, y) = \int \frac{d^3 k}{(2\pi)^{3/2}} \sum_{\bullet=\times,+} e^{i\mathbf{k}\cdot\mathbf{x}} e_{ij}^{\bullet}(\mathbf{k}) h_{\bullet}(t, y; \mathbf{k}) , \quad (13)$$

where $e_{ij}^{\bullet}(\mathbf{k})$ are unitary constant transverse-traceless polarization tensors which form a basis of the two polarization states $\bullet = \times, +$. Since the problem at hand obeys parity symmetry, we shall neglect in the following the distinction between the two graviton polarizations and consider only one of them. We then have to multiply the final results for e.g. particle number or energy density by a factor of two to account for both polarizations.

Here we only consider 4d gravitational waves. The 5d metric has in principle five different spin-2 polarizations. Two of them are the ones discussed here. In addition there are the two helicities of the so-called gravi-vector and a gravi-scalar (see, e.g. [16]). The gravi-vector and the gravi-scalar obey exactly the same propagation equation as the 4d gravitational waves in the bulk, only their boundary conditions are different. In principle they would add to the results obtained here. In this sense our results are conservative, but since the different polarization states do not interact at the linear level they can be calculated independently. These polarizations are expected to contribute on the same level as the two considered here.

The perturbed Einstein equations and the second junction condition lead to the boundary value problem

$$\left[\partial_t^2 + k^2 - \partial_y^2 + \frac{3}{y} \partial_y \right] h(t, y; \mathbf{k}) = 0 \quad \text{in the bulk} \quad (14)$$

and

$$\gamma (v \partial_t + \partial_y) h|_{y_b(t)} = 0 \quad (15)$$

describing the time-evolution of the tensor perturbations as the brane moves through the bulk. We introduce also a second, static brane at position y_s , which requires the additional boundary condition

$$\partial_y h|_{y_s} = 0 . \quad (16)$$

Eq. (14) is the Klein-Gordon equation for a minimally coupled massless mode in AdS_5 , i.e. the operator acting

on h is just the Klein-Gordon operator

$$\square = \frac{1}{\sqrt{-g}} \partial_A [\sqrt{-g} g^{AB} \partial_B] . \quad (17)$$

Equation (15) is a time-dependent boundary condition (BC) coming from the fact that the moving brane acts like a "moving mirror" for the gravitational perturbations. Only in the rest-frame of the brane do we have pure Neumann BC. In a generic frame we have the Lorentz transformed BC which contains a velocity term $v \partial_t$.

We assume that the brane is filled with a perfect fluid such that there are no anisotropic stress perturbations in the brane energy momentum tensor, i.e. there is no coupling of gravitational waves to matter. If this were the case, the r.h.s. of Eq. (15) would not be zero but a term coupling h_{ij} to the matter on the brane, see Eq. (2.25) of [12], would be present.

The analogy to a moving mirror is actually not just a pictorial one. Transverse-magnetic modes of the electromagnetic field in a dynamical ideal, i.e. perfectly conducting, cavity are subject to the very same boundary condition, see, e.g., [17]. In this context, the boundary condition (15) is sometimes referred to as "generalized Neumann" boundary condition, a terminology which we also adopt here. If the cavity is non-perfect, then also in the case of the electromagnetic field, the right hand side of the boundary conditions contains a term describing the interaction of the photon field with cavity material, similar to the anisotropic stress perturbations for the gravitational case considered here. This suggests that a brane with no anisotropic stresses could be termed "ideal brane".

For the tensor perturbations the gravitational action up to second order in the perturbations reads

$$\mathcal{S}_h = 4 \frac{L^3}{2\kappa_5} \int dt \int d^3 k \int_{y_b(t)}^{y_s} \frac{dy}{y^3} [|\partial_t h|^2 - |\partial_y h|^2 - k^2 |h|^2] . \quad (18)$$

One factor of two in the action is due to \mathbb{Z}_2 symmetry while a second factor comes from the two polarizations. As we have shown in [12], the BC's (15,16) are indeed the only ones for which $\delta \mathcal{S}_h = 0$ leads to the free wave equation (14). (In principle also Dirichlet BC's, i.e. h vanishing identically on the brane, lead to a wave equation in the bulk. But besides leaving no room for a non-trivial dynamics of the gravitational waves on the brane, these are not obtained from the Einstein equations in the bulk.)

C. Dynamical Casimir effect approach

The wave equation (14) itself is not time dependent and simply describes the propagation of free modes. It is the time dependence of the BC (15) that sources the non-trivial time-evolution of the perturbations. As it is

well known, such a system of a wave equation and a time-dependent BC lead, within a quantum mechanical formulation, to particle production from vacuum fluctuations. In the context of the photon field perturbed by a moving mirror this goes under the name “dynamical Casimir effect” [5, 6].

In [11, 12] we have extended a formalism which has been successfully employed for the numerical investigation of photon production in dynamical cavities [18, 19, 20] to the RS braneworld scenario. We have studied graviton production by a moving brane, which we call dynamical Casimir effect for gravitons, for a bouncing braneworld scenario.

However, in order to solve the problem, we have neglected the velocity term in the BC (15). The ansatz

$$h = \sum_{\alpha=0}^{\infty} a_{\alpha}(t) e^{-i\omega_{\alpha,k}t} \phi_{\alpha}(t, y) + \text{h.c.}, \quad \omega_{\alpha,k}^2 = k^2 + m_{\alpha}^2(t)$$

then leads to a Sturm–Liouville problem for the instantaneous eigenfunctions $\phi_{\alpha}(t, y)$ consisting of the differential equation

$$\left[-\partial_y^2 + \frac{3}{y} \partial_y \right] \phi_{\alpha}(t, y) = m_{\alpha}^2(t) \phi_{\alpha}(t, y) \quad (19)$$

and Neumann BC’s at both branes. The solutions of (19) respecting Neumann BC’s at both branes are

$$\phi_0(t) = \frac{y_s y_b(t)}{\sqrt{y_s^2 - y_b^2(t)}} \quad (20)$$

$$\phi_n(t, y) = N_n(t) y^2 C_2(m_n(t), y_b(t), y)$$

with

$$C_{\nu}(m, x, y) = Y_1(mx) J_{\nu}(my) - J_1(mx) Y_{\nu}(my). \quad (21)$$

They form a complete orthonormal system with respect to the inner product

$$(\phi_{\alpha}, \phi_{\beta}) = 2 \int_{y_b(t)}^{z_s} \frac{dy}{y^3} \phi_{\alpha}(t, y) \phi_{\beta}(t, y) = \delta_{\alpha\beta} \quad (22)$$

and the completeness relation

$$2 \sum_{\alpha} \phi_{\alpha}(t, y) \phi_{\alpha}(t, \tilde{y}) = \delta(y - \tilde{y}) y^3. \quad (23)$$

The factor two accounts for the \mathbb{Z}_2 symmetry of the bulk.

In [12] we call ϕ_0 and ϕ_n the zero-mode and Kaluza–Klein (KK)- mode solution, respectively. Here ϕ_0 is the massless mode, $m_0 = 0$, which reduces to the usual 3 + 1 - dimensional graviton on the brane. The KK masses $m_n \neq 0$ are determined by the BC at the static brane, see, e.g. [12, 21] for more details.

Due to the completeness and ortho-normality of the functions $\{\phi_{\alpha}\}$ at any instant in time, any general solution of (19) subject to Neumann BC’s can be expanded in these instantaneous eigenfunctions. If we add the term $v\partial_t$ to the boundary condition this feature is lost and we

can no longer expect to find a complete set of instantaneous eigenfunctions.

However, since the entire effect disappears when the velocity tends to zero, neglecting a term which is first order in the velocity seems not to be a consistent approach. This problem prompted us to search for another description allowing us to treat the boundary condition (15) in full.

III. GRAVITON PRODUCTION IN A TIME-DEPENDENT BULK WITH A MOVING BRANE

In this section we introduce a new time coordinate which is chosen such that the velocity term in the boundary condition disappears but the mode equation for the instantaneous eigenfunctions still remains the Bessel equation (19) with its solution given by Eqs. (20) and (21). We then extend the formalism of [12] to this case and shall see that for small velocities our previous results are not modified.

A. A new time coordinate

We introduce new variables $(\tilde{x}^A) = (\tau, \mathbf{x}, z)$ given by

$$\tau(t, y) = t + s(t, y), \quad z = y. \quad (24)$$

The idea is to find a function $s(t, y)$ such that $\tau \rightarrow t$ for all y , when $v \rightarrow 0$ and that the junction condition (15) reduces to a normal Neumann BC in the new variables. We can then use the mode functions (20) and (21) to formulate the problem quantum mechanically. One might first be tempted to make a y -dependent Lorentz transformation to the rest frame of the moving brane, but actually this does not lead to Neumann BC’s in our case as the transformation induces new terms in the metric. We therefore first leave the function $s(t, y)$ completely general and formulate the conditions which have to be satisfied in order for the new BC’s to be purely Neumann.

In (τ, \mathbf{x}, z) -coordinates, the brane trajectory is given by the implicit equation

$$z_b(\tau) = y_b[t(\tau, z_b(\tau))]. \quad (25)$$

Once we have specified the function $s(t, y)$, the new brane trajectory $z_b(\tau)$ can be found. This is done numerically since neither $s(t, y)$ nor the inverse $t(\tau, z)$ of (24) exist in closed form. As in [12] we restrict ourselves to brane motions where asymptotically, i.e. for $t \rightarrow \pm\infty$, the physical brane approaches the Cauchy horizon ($y_b \rightarrow 0$), moving very slowly ($v \rightarrow 0$).

The new metric given by

$$ds^2 = \tilde{g}_{AB}(\tau, z) d\tilde{x}^A d\tilde{x}^B \quad (26)$$

is time dependent and contains non-vanishing cross terms \tilde{g}_{0z} . The explicit expression is given in (A3). We now show that the function $s(t, y)$ can be chosen such that the time-derivative term in the boundary condition disappears.

In the coordinates defined in Eq. (24), the junction condition (15) becomes

$$\left[v(t) \frac{\partial \tau}{\partial t} + \frac{\partial \tau}{\partial y} \right] \partial_\tau h(\tau, z) + \partial_z h(\tau, z) \Big| = [v(t) \{1 + \partial_t s(t, y)\} + \partial_y s(t, y)] \partial_\tau h(\tau, z) + \partial_z h(\tau, z) = 0 \quad \text{at } z = z_b(\tau). \quad (27)$$

In order to obtain Neumann boundary conditions, we require that the term in square brackets vanish at $z_b(\tau)$. This leads to the condition

$$-\frac{\partial_y s(t, y)}{1 + \partial_t s(t, y)} \Big|_{y=y_b(t)} = v(t) \quad (28)$$

for the function $s(t, y)$. Furthermore, we want to maintain the Neumann BC at the static brane $y_s = z_s$. This yields the additional condition for the function $s(t, y)$

$$\partial_y s(t, y)|_{y=y_s} = 0. \quad (29)$$

Hence, if we can find a function $s(t, y)$ which satisfies Eqs. (28) and (29), the junction conditions in the new coordinates reduce to Neumann BC's

$$\partial_z h(\tau, z) = 0 \quad \text{at } z = z_s \quad \text{and } z = z_b(\tau). \quad (30)$$

To find a suitable function $s(t, y)$ we choose the separation ansatz

$$s(t, y) = f(t)\sigma(y) \quad (31)$$

leading to

$$v(t) = -\frac{f(t)\partial_y \sigma(y_b(t))}{1 + (\partial_t f(t))\sigma(y_b(t))}. \quad (32)$$

For the transformation (24) to be regular, we have to require $1 + \partial_t s(t, y) = 1 + \frac{df}{dt}(t)\sigma(y) \neq 0 \quad \forall (t, y)$. If we choose σ such that $\partial_y \sigma(y_b(t))$ is bounded from below, $0 < A < \partial_y \sigma(y_b(t))$, this ansatz ensures the required asymptotics, $f(t) \rightarrow 0$ for $v(t) \rightarrow 0$. In addition we need

$$\partial_y \sigma(y)|_{y=y_s} = 0. \quad (33)$$

The function $f(t)$ is determined by the differential equation

$$\frac{df(t)}{dt} + \frac{1}{v(t)} \frac{\sigma'(y_b(t))}{\sigma(y_b(t))} f(t) + \frac{1}{\sigma(y_b(t))} = 0. \quad (34)$$

A simple choice for $\sigma(y)$ is

$$\sigma(y) = 1 + \frac{1}{\sigma_0} \left(1 - \frac{y}{y_s}\right)^2, \quad \sigma_0 = \text{const.}, \quad \sigma_0 > 1, \quad (35)$$

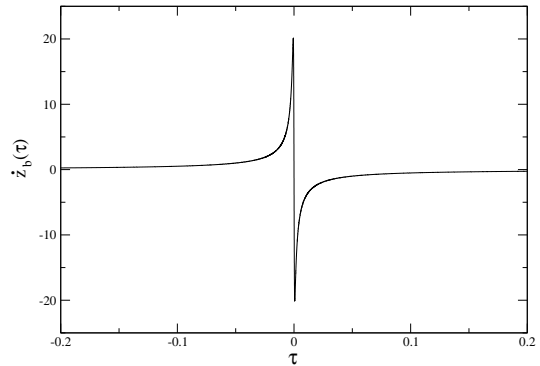


FIG. 2: The velocity in the new coordinates, $\frac{dz_b}{d\tau}$. Note that this is a coordinate velocity, not a physical quantity. It is easy to check that $\tilde{g}_{AB} \frac{d\tilde{x}^A(\tau)}{d\tau} \frac{d\tilde{x}^B(\tau)}{d\tau} < 0$ at all times, hence the physical velocity remains timelike also if $\frac{dz_b}{d\tau}$ becomes larger than 1. The bounce velocity for this case is $v_b = 0.3$.

so that $1 \leq \sigma(y) < 2$. With this, condition (29) is automatically satisfied. In addition, we want the brane collision, i.e. the bounce to happen at the fixed time $\tau = 0$. For this we chose the initial condition

$$f(t = 0) = 0. \quad (36)$$

Since $f(t) \rightarrow 0$ for $v(t) \rightarrow 0$, the transformation (24) satisfies

$$\tau \rightarrow t \quad \text{for } t \rightarrow \pm\infty \quad \text{and } \tau(t = 0, y) = 0. \quad (37)$$

For the first of these equations we use that $v(t) \rightarrow 0$ for $t \rightarrow \pm\infty$ and the form of the differential equation (34).

With (32), $f(0) = 0$ implies that the velocity vanishes at the brane, $v(0_-) = v_b = v(0_+) = 0$. Hence the velocity no longer jumps from a large value v_b to $-v_b$ at the bounce but it evolves very rapidly but smoothly from a high positive value $v_{\text{max}} = v(-\epsilon)$ to a large negative value $-v_{\text{max}} = v(\epsilon)$, $\epsilon > 0$ and small (see Fig. 2). Confirming that the results are independent of the choice of σ_0 is of course a crucial test.

The coordinate transformation maps the problem of a moving brane in a static bulk (1) onto the problem of a brane moving according to (25) in a time-dependent bulk. At first glance a further complication of the problem. Its benefits, however, will become clear in the next sections. The metric is given explicitly in Appendix A.

B. Wave equation

Transforming the Klein-Gordon operator (17) to the new coordinates \tilde{x}^A , we obtain the wave equation

$$\left[g_1(\tau, z) \partial_\tau^2 + g_2(\tau, z) \partial_\tau - 2s_2(\tau, z) \partial_z \partial_\tau + \frac{3}{z} \partial_z - \partial_z^2 + k^2 \right] h(\tau, z) = 0. \quad (38)$$

The definitions of the functions $g_1(\tau, z)$, $g_2(\tau, z)$ and $s_2(\tau, z)$ in terms of the coordinate transformation $s(t, y)$ are given in Appendix A. These functions manifest that the bulk itself is now time-dependent and that the metric is no longer diagonal. In Poincaré coordinates the non-triviality of the time-evolution of the perturbations is purely a consequence of the time-dependent junction condition, no time-dependent functions enter the wave equation (14). Our coordinate transformation which transforms the generalized Neumann BC into a pure Neumann BC, induces explicit time-dependence in the wave equation itself. What is important, however, is that in (38), in the instantaneous rest frame where we neglect time derivatives, we get the operator (19) of the original Bessel equation with normalized solutions (20) and (21). We just have to replace the variables (t, y) by (τ, z) .

Writing the action (18) in terms of the new coordinates yields

$$S = 4 \int d\tau \frac{L^3}{2\kappa_5} \int d^3k \int_{z_b(\tau)}^{z_s} \frac{dz}{z^3} \frac{1}{1+s_1} \times \quad (39)$$

$$\left[g_1 |\partial_\tau h|^2 - 2 s_2 \text{Re} [(\partial_\tau h)(\partial_z h^*)] - |\partial_z h|^2 + k^2 |h|^2 \right].$$

Using the expressions for s_1 , s_2 , g_1 and g_2 given in Appendix A, it is readily shown that the variation of (39), demanding Neumann boundary conditions at the brane positions, leads to the wave equation (38).

In the next subsections we take the action (39) as the starting point to set up the dynamical Casimir effect formulation of graviton production along the same lines as in [11, 12]. For the physical interpretation of gravitons we are using the fact that asymptotically, when the velocity of the brane goes to zero, the action (39) and the wave equation (38) reduce to (18) and (14), respectively. However, in the new coordinates, the junction conditions are always simple Neumann boundary conditions.

C. Mode decomposition and Hamiltonian

As a basis for a mode decomposition we chose the eigenfunctions $\{\phi_\alpha(\tau, z)\}$ obtained by replacing $(t, y) \rightarrow (\tau, z)$ in (20) and (21). As in [12] we call ϕ_0 and ϕ_i the zero-mode and KK mode solution, respectively. For a brane at rest, and hence $\tau = t$, the solutions ϕ_0 and ϕ_i do indeed represent the physical zero mode and the KK modes, see, e.g. [3]. When the brane is moving, however, these solutions are ‘instantaneous modes’, provided that the boundary condition is Neumann. This approach is widely employed in the context of the dynamical Casimir effect, see [18, 19, 20] and references therein. Here, working in the (τ, z) -coordinates, the modes (20) and (21), are proper eigenfunctions respecting the full junction condition which we have reduced to a Neumann BC. At early and late times, i.e. asymptotically $|t| \rightarrow \infty$, where the brane velocity tends to zero, these eigenfunctions agree with the physical eigenfunctions corresponding

to the zero mode and the KK modes. Since the eigenfunctions $\{\phi_\alpha(\tau, z)\}$ form a complete and orthonormal set, and satisfy the correct junction conditions at both branes, we may decompose the graviton field in ϕ_α ’s and the pre-factors $q_{\alpha, \mathbf{k}}(\tau)$ become canonical variables which can then be quantized [12],

$$h(\tau, z, \mathbf{k}) = \sqrt{\frac{\kappa_5}{L^3}} \sum_{\alpha=0}^{\infty} q_{\alpha, \mathbf{k}}(\tau) \phi_\alpha(\tau, z). \quad (40)$$

Our coordinate transformation and the expansion (40) satisfy two major requirements. First, the expansion (40) is consistent with the full junction condition (generalized Neumann BC). This overcomes the problem of our approach in [11, 12]. Secondly, even if at arbitrary times the $q_{\alpha, \mathbf{k}}$ ’s cannot a priori be identified with physical modes, asymptotically, i.e. when the brane moves very slowly, they do represent the independent physical graviton modes. This allows us to introduce a proper notion of particles and vacuum states for asymptotic times. Initial and final vacuum states are then linked by the time-evolution of the $q_{\alpha, \mathbf{k}}$ ’s exactly as in [12].

We divide the wave equation (38) by g_1 in order to isolate the second time derivative and insert the expansion (40). Note that $g_1 \rightarrow 1$ for $|t| \rightarrow \infty$ and for a sufficiently large choice of σ_0 , $g_1 > 0$ at all times. As we shall see below, this is also needed for the Hamiltonian to be positive at all times. Inserting the expansion (40) into (38), multiplying it by ϕ_β and integrating over $2 \int_{z_b(\tau)}^{z_s} dz/z^3$ leads to a system of differential equations for the $q_{\alpha, \mathbf{k}}$ which has the same form as the one of Refs. [11, 12],

$$\ddot{q}_{\alpha, \mathbf{k}}(\tau) + \sum_{\beta} [A_{\beta\alpha}(\tau) \dot{q}_{\beta, \mathbf{k}}(\tau) + B_{\beta\alpha}(\tau) q_{\beta, \mathbf{k}}(\tau)] = 0. \quad (41)$$

The explicit expressions for the time-dependent coupling matrices $A_{\beta\alpha}$ and $B_{\beta\alpha}$ are given by integrals over the bulk which are rather cumbersome. The details can be found in Appendix B. Inserting the expansion (40) into the action (39) we obtain the Lagrangian $L(\tau)$ in terms of the variables $q_{\alpha, \mathbf{k}}(\tau)$. We can then define the canonical momenta $p_{\alpha, \mathbf{k}} = \partial L / \partial \dot{q}_{\alpha, \mathbf{k}}$ from which, by means of a Legendre transformation, we derive the Hamiltonian

$$H(\tau) = \frac{1}{2} \int d^3k \sum_{\alpha\beta} \left[p_{\alpha, \mathbf{k}} E_{\alpha\beta}^{-1} p_{\beta, -\mathbf{k}} + q_{\alpha, \mathbf{k}} \left[\frac{1}{2} (\omega_{\alpha, \mathbf{k}}^2(\tau) + \omega_{\beta, \mathbf{k}}^2(\tau)) \delta_{\alpha\beta} + V_{\alpha\beta} \right] q_{\beta, -\mathbf{k}} - (M_{\beta\alpha} - S_{\beta\alpha}) [q_{\beta, \mathbf{k}} p_{\alpha, \mathbf{k}} + p_{\alpha, \mathbf{k}} q_{\beta, \mathbf{k}}] \right]. \quad (42)$$

The coupling matrices $E_{\alpha\beta}^{-1}$, $V_{\alpha\beta}$, $M_{\beta\alpha}$ and $S_{\beta\alpha}$ are given explicitly in Appendix B. It is important to note that $E_{\alpha\beta}^{-1}$ is positive definite as long as $g_1 > 0$ and $1 + s_1 > 0$, which we have to require for our approach to be consistent. In the old treatment, $E_{\alpha\beta}$ was the identity matrix and the couplings $S_{\beta\alpha}$ and $V_{\alpha\beta}$ were missing. They

are due to the time-dependence of the bulk spacetime in the new coordinates and therefore originate from the term $v\partial_t$ of the boundary condition in Poincaré coordinates. The coupling matrix $M_{\beta\alpha}$ which is also present in our previous treatment comes from the time dependent Neumann BC. Finally, the time dependence of the bulk volume $z_s - z_b(\tau)$, induces the time dependence in the frequency $\omega_{\alpha,k}$ (squeezing effect, see [12]).

All the coupling matrices tend to zero when $v \rightarrow 0$. But we have not been able to show that the new couplings, $E_{\alpha\beta}^{-1} - \delta_{\alpha\beta}$, $V_{\alpha\beta}$ and $S_{\beta\alpha}$ are parametrically smaller than $M_{\beta\alpha}$, e.g. that they are of order v^2 . Therefore, the result that the particle production obtained in our previous treatment [11, 12] is not modified if the velocity is sufficiently low is not evident and has to be checked numerically.

D. Quantum Generation of Gravitons

The quantization procedure goes along the same lines as in [12]. The canonical variables $q_{\alpha,\mathbf{k}}(\tau)$, $p_{\alpha,\mathbf{k}}(\tau)$ and the Hamiltonian $H(\tau)$ are promoted to operators $\hat{q}_{\alpha,\mathbf{k}}(\tau)$, $\hat{p}_{\alpha,\mathbf{k}}(\tau)$ and $\hat{H}(\tau)$, subject to the usual commutation relations. In the Heisenberg picture where the time evolution of an operator \hat{O} is determined by

$$\dot{\hat{O}}(\tau) = i[\hat{H}(\tau), \hat{O}(\tau)] + \left(\frac{\partial \hat{O}(\tau)}{\partial \tau} \right)_{\text{expl}},$$

the operators $\hat{q}_{\alpha,\mathbf{k}}(\tau)$ and $\hat{p}_{\alpha,\mathbf{k}}(\tau)$ satisfy the same Hamiltonian equations of motion as their classical counterparts, i.e.

$$\dot{q}_{\alpha,\mathbf{k}} = \frac{\partial H}{\partial p_{\alpha,\mathbf{k}}}, \quad \dot{p}_{\alpha,\mathbf{k}} = -\frac{\partial H}{\partial q_{\alpha,\mathbf{k}}} \quad (43)$$

Remember that we assume that asymptotically, $|t| \rightarrow \infty$, the brane is at rest, i.e. the brane velocity vanishes and both coordinate systems agree, $\tau = t$. We extend this notion of asymptotic behavior by introducing two times, t_{in} and t_{out} , and we shall assume that the brane is at rest for $t \leq t_{\text{in}}$ and $t \geq t_{\text{out}}$, respectively. This corresponds to a scenario where the motion of the brane is switched on and off at finite times. Such a brane dynamics may seem rather artificial from a physical point of view, but what is important for us is that before t_{in} and after t_{out} no significant particle creation takes place. Numerically, we test this by varying t_{in} and t_{out} and choosing them large enough so that the particle number is independent of the value chosen.

In the (τ, z) -coordinates, the brane is then at rest for times $\tau \equiv t \leq \tau_{\text{in}} \equiv t_{\text{in}}$ and $\tau \equiv t \geq \tau_{\text{out}} \equiv t_{\text{out}}$, respectively. When the brane velocity is zero, the matrix $E_{\alpha\beta}(\tau)$ defined in Appendix B becomes the identity, $E_{\alpha\beta}(\tau) \rightarrow_{|\tau| \rightarrow \infty} \delta_{\alpha\beta}$, and all other matrices which represent the coupling terms vanish identically in this limit.

Consequently, for asymptotic times the Hamiltonian reduces to the familiar form of a collection of independent harmonic oscillators,

$$\hat{H}^{\text{in/out}} = \frac{1}{2} \int d^3k \sum_{\alpha} \left[|\hat{p}_{\alpha,\mathbf{k}}|^2 + \left(\omega_{\alpha,k}^{\text{in/out}} \right)^2 |\hat{q}_{\alpha,\mathbf{k}}|^2 \right] \quad (44)$$

with

$$\hat{p}_{\alpha,\mathbf{k}} = \dot{\hat{q}}_{\alpha,-\mathbf{k}}. \quad (45)$$

We have introduced the notation

$$\omega_{\alpha,k}^{\text{in}} \equiv \omega_{\alpha,k}(\tau \leq \tau_{\text{in}}), \quad \omega_{\alpha,k}^{\text{out}} \equiv \omega_{\alpha,k}(\tau \geq \tau_{\text{out}}). \quad (46)$$

Following [12], we decompose $\hat{q}_{\alpha,\mathbf{k}}$ in creation and annihilation operators,

$$\hat{q}_{\alpha,\mathbf{k}}(\tau) = \sum_{\beta} \frac{1}{\sqrt{2\omega_{\beta,k}^{\text{in}}}} \left[\hat{a}_{\beta,\mathbf{k}}^{\text{in}} \epsilon_{\alpha,k}^{(\beta)}(\tau) + \hat{a}_{\beta,-\mathbf{k}}^{\text{in}\dagger} \epsilon_{\alpha,k}^{(\beta)*}(\tau) \right], \quad (47)$$

which are defined via $\hat{a}_{\alpha,\mathbf{k}}^{\text{in}}|0, \text{in}\rangle = 0 \quad \forall \quad \alpha, \mathbf{k}$. The initial vacuum state $|0, \text{in}\rangle$ is the ground state of the Hamiltonian (44) for times $\tau \leq \tau_{\text{in}}$. This initial state is linked to the final vacuum state defined by $\hat{a}_{\alpha,\mathbf{k}}^{\text{out}}|0, \text{out}\rangle = 0; \forall \alpha, \mathbf{k}$, by means of a Bogoliubov transformation (see [12])

$$\alpha_{\beta,\mathbf{k}}^{\text{out}} = \sum_{\alpha} \left[\mathcal{A}_{\alpha\beta,k}(\tau_{\text{out}}) \hat{a}_{\alpha,\mathbf{k}}^{\text{in}} + \mathcal{B}_{\alpha\beta,k}^*(\tau_{\text{out}}) \hat{a}_{\alpha,-\mathbf{k}}^{\text{in}\dagger} \right] \quad (48)$$

which determines the number of produced gravitons (for each polarization)

$$N_{\alpha,k}^{\text{out}} = \sum_{\beta} |\mathcal{B}_{\beta\alpha,k}(\tau_{\text{out}})|^2. \quad (49)$$

As we have discussed in detail in [12], the graviton number after the time τ_{out} , (49), represents a physically meaningful quantity.

IV. NUMERICAL RESULTS

In order to solve the equations of motion (41) numerically, we transform the system to a first order system and introduce a mass cutoff, n_{max} , i.e. we neglect all modes with masses higher than $m_{n_{\text{max}}}$, in other words $q_{\alpha} = 0$ for $\alpha > n_{\text{max}}$, along the lines explained in detail in Ref. [12]. Modes close to this cutoff are of course seriously affected by it as is seen in Figs. 3, 4 and 5. We have tested the stability of the results for modes $n \ll n_{\text{max}}$ by varying the cutoff. The stability of the zero mode is illustrated in the lower panel of Figs. 3 and 4. Typically modes with $n \lesssim 0.7n_{\text{max}}$ can be trusted. An indication for this is also the Bogoliubov test shown in Fig. 6 and discussed in Ref. [12].

The first order system is given explicitly in Appendix B3 and differs from the original one in [12] only

by additional mode couplings. We have compared our new results with those of Ref. [11, 12] and find excellent agreement at low velocity, $v_b \lesssim 0.1$. This is illustrated in Figs. 3 and 4. At bounce velocities $v_b \gtrsim 0.5$ we do find differences as expected, but these results cannot be taken literally since for these velocities the low energy evolution of the scale factor adopted in this work is no longer sufficient. We will present the full high velocity results in a forthcoming paper [15].

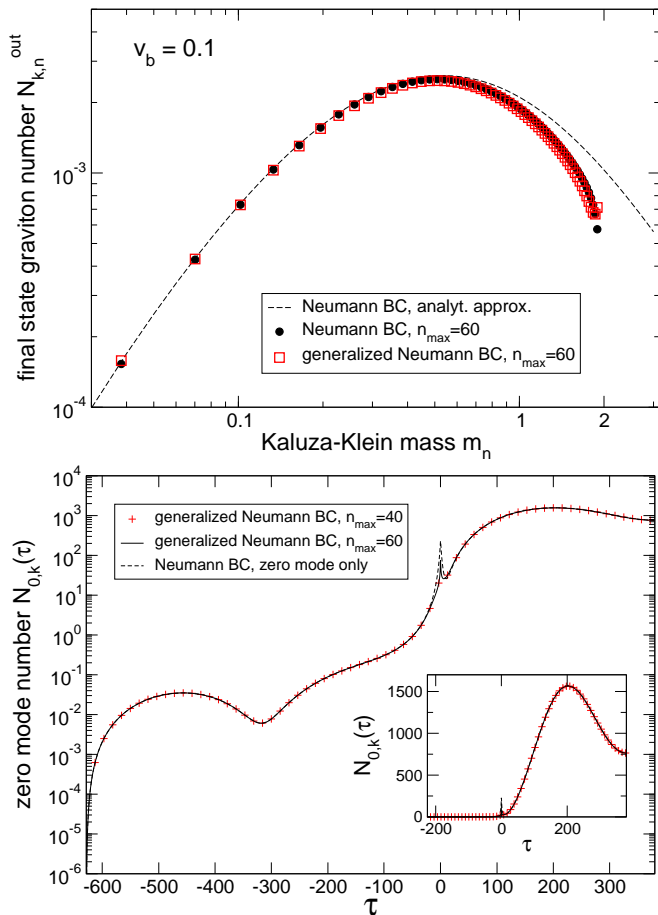


FIG. 3: The final graviton spectrum for three-momentum $k = 0.01$, brane separation $y_s = 100$ and bounce velocity $v_b = 0.1$. The top panel shows the final KK mode spectrum and the lower panel depicts the time evolution of the zero mode. What we plot here is a kind of instantaneous particle number (see Appendix C of [12]). The numerical result for the KK spectrum is compared with the old one (shown in Fig. 13 of [12]). Like there, lengths are in units of L and momenta/masses in the units of L^{-1} . For low velocities $v_b \leq 0.1$ the new spectra (generalized Neumann BC) are identical with the old ones (Neumann BC) within the numerical error which are estimated by the Bogoliubov test (see Appendix). $N_{0,k}(\tau)$ is shown for two cut-off parameters n_{max} to underline stability of the solution.

The agreement between the old results for pure Neumann boundary conditions and the new ones with the generalized Neumann boundary conditions is similar for

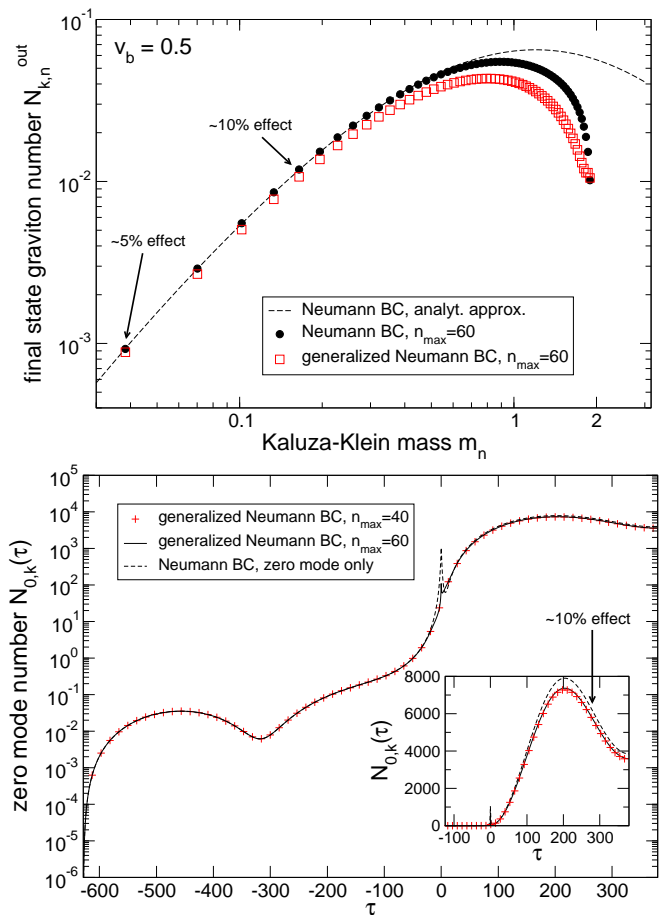


FIG. 4: As Figure 3 but for $v_b = 0.5$. For this velocity we do see a difference of about 10% between the previous, inconsistent approach and the new generalized Neumann BC for both, the KK modes as well as the zero mode. Again, the 4d graviton number is shown for two cut-off parameters n_{max} to indicate numerical stability. .

other values of y_s and k .

In Fig. 5 we show the KK spectra for $v_b = 0.1$ and $v_b = 0.3$ for the wave number $k = 0.1$ and position of the static brane, $y_s = 10$. In this case, the analytic approximation derived in Ref. [12] which is valid for $m_n < 1$ can only be trusted for the first two modes. The slight difference between the old and the new spectra towards the end, i.e. for $m_n > 10$, is due to changes how we numerically evolve the solutions through the bounce (see Appendix C). This affects the sensitivity of the solutions to the cut-off. What we observe here as a slight bending of the spectrum for generalized Neumann BC's is also found in our previous approach if we increase the number of modes; compare to the $n_{\text{max}} = 100$ results shown in Fig. 15 of [12] and the discussion related to Fig. 25 of [12]. The drop in the final part of the spectrum is just an artefact of the finite cut-off (see [12] for a detailed discussion).

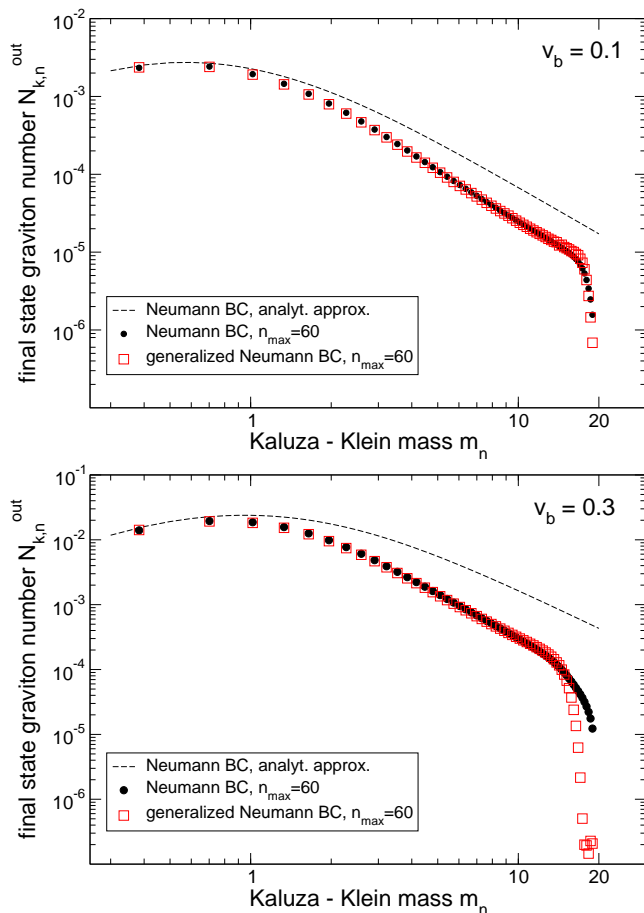


FIG. 5: Final graviton spectra for three-momentum $k = 0.1$ and brane separation $y_s = 10$ for the bounce velocities $v_b = 0.1$ and 0.3 . Again, the new (generalized Neumann BC) numerical results are compared with the ones of the previous inconsistent approach (Neumann BC), see Fig. 15 of [12]. and the agreement is excellent in the regime $m_n < 13$, where the numerics can be trusted.

V. CONCLUSIONS

In this paper we have derived a method to calculate graviton production in bouncing AdS₅ braneworlds by the dynamical Casimir effect taking into account the full generalized Neumann boundary condition. We have achieved this by transforming to a new time coordinate, in which the generalized Neumann BC become ordinary Neumann BC. We have shown numerically that for low bounce velocities, $v_b \lesssim 0.1$, the number of generated particles agrees with the one from the simpler treatment which neglects the velocity term in the boundary condition. Since this term is of first order in the velocity, we believe that our result is not obvious. Furthermore, the method developed in this work can be used to calculate particle creation for branes moving at arbitrarily high velocities. In this case, one will have to take into account the modification of the Friedmann equation at

high energy, $HL \gtrsim 1$. This is the goal of a forthcoming paper [15].

In this work we have not derived new physical results, but we have developed a new, fully consistent method to calculate graviton production due to the motion of a braneworld. Our method overcomes a shortcoming of our previous treatment [11, 12], and we have verified that at low brane velocity, $v_b \lesssim 0.3$ the previous results are not affected.

Acknowledgment

This work is supported by the Swiss National Science Foundation. The numerical simulations have been carried out on the Myrinet cluster of Geneva University. RD thanks the Galileo Galilei Institute of theoretical physics, where this work was finalized, for hospitality.

APPENDIX A: THE COORDINATE TRANSFORMATION

The Jacobian \mathbf{T} of the transformation

$$(t, y) \mapsto (\tau = t + s(t, y), z = y)$$

reads

$$\mathbf{T} = \frac{\partial(\tau, \mathbf{x}, z)}{\partial(t, \mathbf{x}, y)} = \begin{pmatrix} 1 + \partial_t s & 0 & 0 & 0 & \partial_y s \\ 0 & 1 & 0 & 0 & 0 \\ 0 & 0 & 1 & 0 & 0 \\ 0 & 0 & 0 & 1 & 0 \\ 0 & 0 & 0 & 0 & 1 \end{pmatrix}, \quad (\text{A1})$$

and its inverse is

$$\mathbf{T}^{-1} = \frac{\partial(t, \mathbf{x}, y)}{\partial(\tau, \mathbf{x}, z)} = \begin{pmatrix} \frac{1}{1 + \partial_t s} & 0 & 0 & 0 & \frac{-\partial_y s}{1 + \partial_t s} \\ 0 & 1 & 0 & 0 & 0 \\ 0 & 0 & 1 & 0 & 0 \\ 0 & 0 & 0 & 1 & 0 \\ 0 & 0 & 0 & 0 & 1 \end{pmatrix}.$$

Under this coordinate transformation the AdS₅ metric in Poincaré coordinates given in (1) transforms to

$$\begin{aligned} \tilde{g}_{AB} d\tilde{x}^A d\tilde{x}^B &= ((\mathbf{T}^{-1})^T g \mathbf{T}^{-1})_{AB} d\tilde{x}^A d\tilde{x}^B \\ &= \frac{L^2}{z^2} \left[\frac{1}{(1 + s_1(\tau, z))^2} \left(-d\tau^2 \right. \right. \\ &\quad \left. \left. + 2s_2(\tau, z) d\tau dz + g_1(\tau, z) dz^2 \right) + \delta_{ij} dx^i dx^j \right]. \end{aligned} \quad (\text{A2})$$

We introduce the functions

$$s_1(\tau, z) = (\partial_t s)(t(\tau, z), z) \quad (\text{A3})$$

$$s_2(\tau, z) = (\partial_z s)|_{t=\text{const}}(t(\tau, z), z) \quad (\text{A4})$$

$$s_{11}(\tau, z) = (\partial_t^2 s)(t(\tau, z), z) \quad (\text{A5})$$

$$s_{22}(\tau, z) = (\partial_z^2 s)|_{t=\text{const}}(t(\tau, z), z) \quad (\text{A6})$$

and

$$g_1(\tau, z) = (1 + s_1(\tau, z))^2 - s_2(\tau, z)^2 \quad (\text{A7})$$

$$g_2(\tau, z) = s_{11}(\tau, z) - s_{22}(\tau, z) + \frac{3}{z}s_2(\tau, z), \quad (\text{A8})$$

of which g_1 and g_2 will be used in Appendix B. The determinant is

$$\tilde{g} = \det(\tilde{g}_{AB}) = - \left(\frac{L}{z}\right)^{10} \frac{1}{(1 + s_1(\tau, z))^2}. \quad (\text{A9})$$

APPENDIX B: DETAILS ON EVOLUTION EQUATIONS

1. Wave equation

The coupling matrices which determine the mode evolution equation (41) are given in terms of the following bulk integrals:

$$A_{\alpha\beta}(\tau) = 2 \int_{z_b(\tau)}^{z_s} \frac{dz}{z^3} \left[2\dot{\phi}_\alpha + \frac{g_2(\tau, z)}{g_1(\tau, z)}\phi_\alpha(\tau, z) - \frac{2s_2(\tau, z)}{g_1(\tau, z)}\phi'_\alpha(\tau, z) \right] \phi_\beta(\tau, z) \quad (\text{B1})$$

$$B_{\alpha\beta}(\tau) = 2 \int_{z_b(\tau)}^{z_s} \frac{dz}{z^3} \left[\ddot{\phi}_\alpha(\tau, z) + \frac{g_2(\tau, z)}{g_1(\tau, z)}\dot{\phi}_\alpha(\tau, z) - \frac{2s_2(\tau, z)}{g_1(\tau, z)}\phi'_\alpha(\tau, z) + \frac{\omega_{\alpha,k}^2(\tau)}{g_1(\tau, z)}\phi_\alpha(\tau, z) \right] \phi_\beta(\tau, z) \quad (\text{B2})$$

with

$$\omega_{\alpha,k}(\tau) = \sqrt{m_\alpha^2(\tau) + k^2}. \quad (\text{B3})$$

The over-dot denotes the derivative w.r.t. the time τ and a prime stands for the derivative w.r.t. the coordinate z . Compared to our former work [12], the present problem is more complicated due to the additional couplings which are caused by the time-dependence of the bulk space-time. Also the Lagrangian and Hamiltonian equations for $q_{\alpha,k}$ are more complicated. Furthermore, the functions s_1, s_2, g_1 and g_2 are only known numerically. This induces additional numerical difficulties. Note also that it is important that g_1 does not pass through zero for these integrals to be well defined, hence $g_1(\tau, z) > 0 \forall \tau, z$. This is, however, easily achieved with our ansatz (31, 35) for $s(t, y)$ if we choose σ_0 sufficiently large.

2. Lagrangian and Hamiltonian formulation

Inserting the expansion (40) into the action (39) leads (for each of the polarizations) to the Lagrangian

$$L(\tau) = \frac{1}{2} \int d^3k \sum_{\alpha\beta} \left[E_{\alpha\beta} \dot{q}_{\alpha,\mathbf{k}} \dot{q}_{\beta,-\mathbf{k}} + (\mathcal{M}_{\alpha\beta} - \mathcal{K}_{\alpha\beta})(q_{\alpha,\mathbf{k}} \dot{q}_{\beta,-\mathbf{k}} + q_{\alpha,-\mathbf{k}} \dot{q}_{\beta,\mathbf{k}}) + (\mathcal{N}_{\alpha\beta} - \mathcal{P}_{\alpha\beta} - \mathcal{Q}_{\alpha\beta} - \omega_{\alpha\beta,k}^2) q_{\alpha,\mathbf{k}} q_{\beta,-\mathbf{k}} \right]$$

containing several time-dependent coupling terms. In detail, these read

$$\begin{aligned} E_{\alpha\beta}(\tau) &= 2 \int_{z_b(\tau)}^{z_s} \frac{dz}{z^3} \frac{g_1(\tau, z)}{1 + s_1(\tau, z)} \phi_\alpha(\tau, z) \phi_\beta(\tau, z) \\ \mathcal{M}_{\alpha\beta}(\tau) &= 2 \int_{z_b(\tau)}^{z_s} \frac{dz}{z^3} \frac{g_1(\tau, z)}{1 + s_1(\tau, z)} \dot{\phi}_\alpha(\tau, z) \phi_\beta(\tau, z) \\ \mathcal{N}_{\alpha\beta}(\tau) &= 2 \int_{z_b(\tau)}^{z_s} \frac{dz}{z^3} \frac{g_1(\tau, z)}{1 + s_1(\tau, z)} \dot{\phi}_\alpha(\tau, z) \dot{\phi}_\beta(\tau, z) \\ \mathcal{K}_{\alpha\beta}(\tau) &= 2 \int_{z_b(\tau)}^{z_s} \frac{dz}{z^3} \frac{s_2(\tau, z)}{1 + s_1(\tau, z)} \phi'_\alpha(\tau, z) \phi_\beta(\tau, z) \\ \mathcal{P}_{\alpha\beta}(\tau) &= 2 \int_{z_b(\tau)}^{z_s} \frac{dz}{z^3} \frac{s_2(\tau, z)}{1 + s_1(\tau, z)} [\dot{\phi}_\alpha(\tau, z) \phi'_\beta(\tau, z) + \phi'_\alpha(\tau, z) \dot{\phi}_\beta(\tau, z)] \\ \mathcal{Q}_{\alpha\beta}(\tau) &= \int_{z_b(\tau)}^{z_s} \frac{dz}{z^3} \frac{s_1'(\tau, z)}{(1 + s_1(\tau, z))^2} [\phi_\alpha(\tau, z) \phi'_\beta(\tau, z) + \phi'_\alpha(\tau, z) \phi_\beta(\tau, z)] \\ \omega_{\alpha\beta,k}^2(\tau) &= 2 \left[\frac{1}{2} (m_\alpha^2(\tau) + m_\beta^2(\tau)) + k^2 \right] \times \int_{z_b(\tau)}^{z_s} \frac{dz}{z^3} \frac{\phi_\alpha(\tau, z) \phi_\beta(\tau, z)}{1 + s_1(\tau, z)}. \end{aligned}$$

Since we require $g_1(\tau, z) > 0$ and $1 + s_1(\tau, z) > 0$, the matrix $E_{\alpha\beta}$ is positive definite. This is important for the above Lagrangian to lead to consistent second order equations of motion for the variables $q_{\alpha,\mathbf{k}}$ (no ghosts).

The equation of motion for the canonical variables obtained from the Euler–Lagrange equations become

$$\begin{aligned} \sum_{\alpha} \left[E_{\alpha\gamma} \ddot{q}_{\alpha,\mathbf{k}} + \dot{E}_{\alpha\gamma} \dot{q}_{\alpha,\mathbf{k}} + (\dot{\mathcal{M}} - \dot{\mathcal{K}})_{\alpha\gamma} q_{\alpha,\mathbf{k}} + [(\mathcal{M} - \mathcal{K})_{\alpha\gamma} - (\mathcal{M} - \mathcal{K})_{\gamma\alpha}] \dot{q}_{\alpha,\mathbf{k}} - (\mathcal{N}_{\alpha\gamma} - \mathcal{P}_{\alpha\gamma} - \mathcal{Q}_{\alpha\gamma} - \omega_{\alpha\gamma,k}) q_{\alpha,\mathbf{k}} \right] &= 0. \quad (\text{B4}) \end{aligned}$$

Note that all the matrices introduced above apart from $E_{\alpha\beta}$ tend to zero when $v \rightarrow 0$, i.e. for $|\tau| \rightarrow \infty$. In this limit $E_{\alpha\beta}$ tends to $\delta_{\alpha\beta}$ so that Eq. (B4) becomes the free, uncoupled mode evolution equation in this limit as is expected. Introducing the canonically conjugate

variables

$$p_{\alpha,\mathbf{k}} = \frac{\partial L}{\partial \dot{q}_{\alpha,\mathbf{k}}} = \sum_{\beta} [E_{\alpha\beta} \dot{q}_{\beta,-\mathbf{k}} + (\mathcal{M}_{\beta\alpha} - \mathcal{K}_{\beta\alpha}) q_{\beta,-\mathbf{k}}] \quad (\text{B5})$$

leads by means of a Legendre transformation to the Hamiltonian (42) with coupling matrices

$$V_{\alpha\beta}(\tau) = 2 \int_{z_b(\tau)}^{z_s} \frac{dz}{z^3} \frac{1}{1+s_1} \left[\left(\frac{s_2^2}{g_1} - s_1 \right) \phi'_{\alpha}(\tau, z) \phi'_{\beta}(\tau, z) - k^2 s_1(\tau, z) \phi_{\alpha}(\tau, z) \phi_{\beta}(\tau, z) \right] \quad (\text{B6})$$

$$M_{\alpha\beta}(\tau) = 2 \int_{z_b(\tau)}^{z_s} \frac{dz}{z^3} \dot{\phi}_{\alpha}(\tau, z) \phi_{\beta}(\tau, z) \quad (\text{B7})$$

$$S_{\alpha\beta}(\tau) = 2 \int_{z_b(\tau)}^{z_s} \frac{dz}{z^3} \frac{s_2}{g_1} \phi'_{\alpha}(\tau, z) \phi_{\beta}(\tau, z). \quad (\text{B8})$$

Thereby $E_{\alpha\beta}^{-1}$ is the inverse of $E_{\alpha\beta}$, i.e.

$$E_{\alpha\beta}^{-1} = 2 \int_{z_b(\tau)}^{z_s} \frac{dz}{z^3} \frac{1+s_1(\tau, z)}{g_1(\tau, z)} \phi_{\alpha}(\tau, z) \phi_{\beta}(\tau, z). \quad (\text{B9})$$

The Hamilton equations

$$\dot{q}_{\alpha,\mathbf{k}} = \frac{\partial H}{\partial p_{\alpha,\mathbf{k}}}, \quad \dot{p}_{\alpha,\mathbf{k}} = -\frac{\partial H}{\partial q_{\alpha,\mathbf{k}}} \quad (\text{B10})$$

then provide the equations of motion for the variables $q_{\alpha,\mathbf{k}}$ and $p_{\alpha,\mathbf{k}}$.

Using certain relations of the coupling matrices following from the completeness (23) and ortho-normality (22) of the functions ϕ_{α} and the properties of the functions s_1, s_2, s_{11} and s_{22} one can show that the three systems of equations (41), (B4) and the Hamilton equations (B10) are consistent with each other, i.e. one system follows from the other one. This seems to be at first sight a rather trivial statement but we have to remind the reader that this is not the case in our previous work [11, 12] as we have discussed in detail in Section II. D of Ref. [12]. The new coupling matrices $V_{\alpha\beta}$, $S_{\alpha\beta}$ and $E_{\alpha\beta} - \delta_{\alpha\beta}$ are missing in our previous work. Even though they do become very small when the brane velocity becomes small, it is not evident that these new terms must be smaller than e.g. $M_{\alpha\beta}$, which also tends to zero with v . In other words, it is not straight forward to show that these contributions are, e.g., of order v^2 .

3. Bogoliubov coefficients

Performing the quantization as in Ref. [12] we again transform to a first order system of equation. In the new coordinates the system of equations (3.34), (3.35) of [12]

is replaced by

$$\begin{aligned} \dot{\xi}_{\alpha}^{(\gamma)}(\tau) &= \sum_{\beta} \left\{ - \left[ia_{\alpha\beta}^{+}(\tau) + c_{\alpha\beta}^{-}(\tau) \right] \xi_{\beta}^{(\gamma)}(\tau) \right. \\ &\quad \left. + \left[ia_{\alpha\beta}^{-}(\tau) - c_{\alpha\beta}^{+}(\tau) \right] \eta_{\beta}^{(\gamma)}(\tau) \right\} \quad (\text{B11}) \end{aligned}$$

$$\begin{aligned} \dot{\eta}_{\alpha}^{(\gamma)}(\tau) &= \sum_{\beta} \left\{ \left[ia_{\alpha\beta}^{+}(\tau) - c_{\alpha\beta}^{-}(\tau) \right] \eta_{\beta}^{(\gamma)}(\tau) \right. \\ &\quad \left. - \left[ia_{\alpha\beta}^{-}(\tau) + c_{\alpha\beta}^{+}(\tau) \right] \xi_{\beta}^{(\gamma)}(\tau) \right\} \quad (\text{B12}) \end{aligned}$$

where

$$\begin{aligned} a_{\alpha\beta}^{\pm}(\tau) &= \frac{1}{2} \left[\omega_{\beta,k}^{\text{in}} E_{\alpha\beta}^{-1}(\tau) \pm \frac{1}{\omega_{\alpha,k}^{\text{in}}} \left(\frac{1}{2} (\omega_{\alpha,k}^2(\tau) \right. \right. \\ &\quad \left. \left. + \omega_{\beta,k}^2(\tau) \right) \delta_{\alpha\beta} + V_{\alpha\beta}(\tau) \right] \quad (\text{B13}) \end{aligned}$$

$$\begin{aligned} c_{\alpha\beta}^{\pm}(\tau) &= \frac{1}{2} \left[M_{\beta\alpha}(\tau) - S_{\beta\alpha}(\tau) \right. \\ &\quad \left. \pm \frac{\omega_{\beta,k}^{\text{in}}}{\omega_{\alpha,k}^{\text{in}}} (M_{\alpha\beta}(\tau) - S_{\alpha\beta}(\tau)) \right]. \quad (\text{B14}) \end{aligned}$$

(Note that in Ref. [12] a factor of two is missing in the expression for M_{ij}^{N} in Eq. (B8), a simple misprint.)

APPENDIX C: NUMERICS

To compute the graviton spectra we have adapted the code described in Ref. [12] to the new problem. Apart from calculating the new coupling matrices we also have to solve the differential equation (34) numerically to calculate the coordinate transformation and its inverse in order to determine $z_b(\tau)$ via the implicit equation (25) as well as the functions $s_1(\tau, z)$, $s_2(\tau, z)$, $g_1(\tau, z)$ and $g_2(\tau, z)$ which enter the integrals for the coupling matrices. Due to this implicit nature of the coordinate transformation, the calculation of these coupling matrices is numerically significantly more involved than in our previous approach.

As in [12], splines are used to interpolate the various matrix elements between time steps. The time steps used to produce the splines are not uniformly distributed but carefully selected to take into account the steepness of the time dependence of the couplings. Close to the bounce we use very short time steps to produce the splines ($\sim 10^{-6}$) while far away we can increase the step up to 0.2 (in units of L). Furthermore, due to the complex time dependence of some of the couplings very close to the bounce, exact integration of the matrix elements when propagating the solutions through the bounce is necessary in order to obtain satisfactory accuracy for large KK masses as in Fig. 5. In this way the bounce is taken into account as accurate as possible. This affects the speed of convergence of the solutions w.r.t. n_{max} , leading to the behavior described below Fig. 5.

As an indicator for the accuracy of our calculations we use the Bogoliubov test as described in Appendix D of [12] (Eq. (D6)). This is presented in Fig. 6 for the $v_b = 0.3$ result given in Fig. 5. The quantity denoted by 'Bogoliubov test' and shown as solid line in Fig. 6 should ideally vanish. Given the complex nature of the numerical problem, the accuracy of the results is satisfactory for $m_n \lesssim 10/L$.

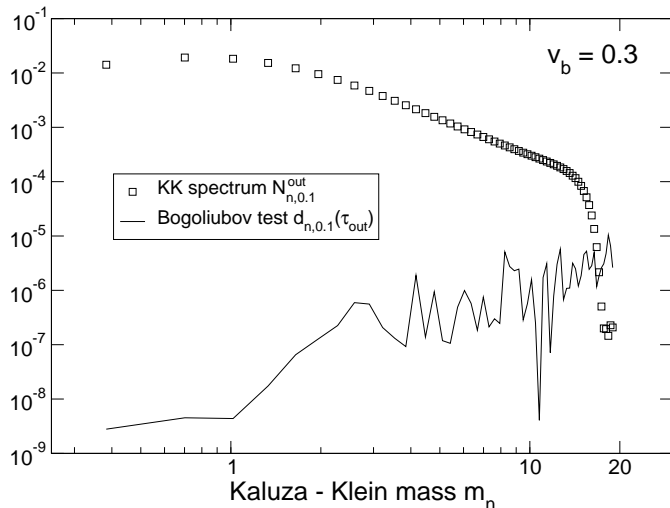


FIG. 6: Comparison of the final KK spectrum $N_{n,0.1}^{\text{out}}$ and the corresponding quantity $d_{n,0.1}(\tau_{\text{out}})$ given in Eq. (D6) of [12]. The quantity $d_{n,0.1}(\tau_{\text{out}})$ is supposed to vanish identically, see [12]. The comparison is a measure for the accuracy of the $v_b = 0.3$ result depicted in Fig. 5. In the region of the spectrum which is free from numerical artefacts, i.e. no dependence on cut-off n_{max} , $d_{n,0.1}(\tau_{\text{out}})$ is at least about two orders of magnitude smaller than the physically relevant quantity $N_{n,0.1}^{\text{out}}$ indicating a satisfactory accuracy.

-
- [1] R. Maartens, Living Rev. Rel. **7**, 7 (2004).
[e-Print: arXiv:gr-qc/0312059]
- [2] R. Durrer, *Braneworlds*, at the XI Brazilian School of Cosmology and Gravitation, Edt. M. Novello and S.E. Perez Bergliaffa, AIP Conference Proceedings 782 (2005).
[e-Print: arXiv:hep-th/0507006]
- [3] L. Randall and R. Sundrum, Phys. Rev. Lett. **83**, 3370 (1999).
[e-Print: arXiv:hep-th/9905221]
- [4] L. Randall and R. Sundrum, Phys. Rev. Lett. **83**, 4690 (1999).
[e-Print: arXiv:hep-th/9906064]
- [5] M. Bordag, *Quantum Field Theory under the Influence of External Conditions* (Teuber, Stuttgart, 1996).
- [6] V. V. Dodonov, Adv. Chem. Phys. **119**, 309, (2001). [e-Print: arXiv:quant-ph/0106081]
- [7] D. S. Gorbunov, V. A. Rubakov, and S. M. Sibiryakov, JHEP **10**, 015 (2001).
[e-Print: arXiv:hep-th/0108017]
- [8] T. Kobayashi, H. Kudoh, and T. Tanaka, Phys. Rev. D **68**, 044025 (2003);
[e-Print: arXiv:gr-qc/0305006]
T. Kobayashi and T. Tanaka, Phys. Rev. D **71**, 124028 (2005);
[e-Print: arXiv:hep-th/0505065]
T. Kobayashi and T. Tanaka, Phys. Rev. D **73**, 044005 (2006).
[e-Print: arXiv:hep-th/0511186]
- [9] K. Koyama, JCAP **0409**, 010 (2004).
[e-Print: arXiv:astro-ph/0407263]
- [10] S. Seahra, Phys. Rev. D **74**, 044010 (2006).
[e-Print: arXiv:hep-th/0602194v2]
- [11] R. Durrer and M. Ruser, Phys. Rev. Lett. **99**, 071601 (2007).
[e-Print: arXiv:0704.0756]
- [12] M. Ruser and R. Durrer, Phys. Rev. D **76**, 104014 (2007).
[e-Print: arXiv:0704.0790]

- [13] J. Khoury, P. Steinhardt and N. Turok, Phys. Rev. Lett. **92**, 031302 (2004),
[e-print: arXiv:hep-th/0307132]
Phys. Rev. Lett. **91** 161301 (2003).
[e-print: arXiv:astro-ph/0302012]
- [14] R. Durrer, M. Ruser, M. Vonlanthen and P. Wittwer, Proceedings Spanish GR meeting, (2009).
[e-print: arXiv:astro-ph/0902.0872]
- [15] R. Durrer, M. Ruser, M. Vonlanthen and P. Wittwer, in preparation.
- [16] C. Cartier and R. Durrer, Phys. Rev. **D71**, 064022 (2005).
[e-print: arXiv:hep-th/0409287v2]
- [17] M. Crocce, D. A. R. Dalvit, F. D. Mazzitelli, Phys. Rev. **A66**, 033811 (2002).
[e-print: arXiv:quant-ph/0205104]
- [18] M. Ruser, Opt. B: Quantum Semiclass Opt. **7**, S100 (2005).
[e-print: arXiv:quant-ph/0408142]
- [19] M. Ruser, Phys. Rev. A **73**, 043811 (2006).
[e-print: arXiv:quant-ph/0509030]
- [20] M. Ruser, J. Phys. A **39** (2006) 6711. [e-print: arXiv:quant-ph/0603097]
- [21] C. Cartier, R. Durrer and M. Ruser, Phys. Rev. **D72**, 104018 (2005).
[e-print: arXiv:hep-th/0510155]
- [22] http://www.gnu.org/software/gsl/manual/html_node/Interpolation-Types.html